

Indium, chromium and nickel-modified eutectic Sn–0.7 wt% Cu lead-free solder rapidly solidified from molten state

Rizk Mostafa Shalaby¹

Received: 15 March 2015 / Accepted: 24 May 2015 / Published online: 3 June 2015
© Springer Science+Business Media New York 2015

Abstract Sn–Cu eutectic modified by minor In, Cr and Ni additions are one of the major alternatives to lead-free solders. The results show that nanostructured solders produced by rapid solidification are dependent on melting properties and the melting temperature. It is found that the In, Cr or Ni addition has the effect of suppressing the formation of eutectic rapidly solidified Sn–0.7Cu alloy. The results indicated that the melting temperatures (T_m) of Sn–0.7Cu are modified to lower temperature by In, Cr and Ni additions. The formation of new intermetallic compounds such as In_3Sn , Cu_6Sn_5 , $Cu_{10}Sn_3$, and $NiSn$ are more uniformly distributed inside Sn-rich phase effectively enhancing the hardness and creep resistance of the eutectic Sn–0.7Cu solder joint at room temperature. The results of these tests are consistent with positive effect of the In, Cr and Ni in enhancing the performance of the eutectic Sn–0.7Cu solder as a practical to lead-free solder.

1 Introduction

The solidification of metals is complicated by solute partition at the interface between solids and liquids points. The time enough for the diffusion of atoms is the basis for the requirements that solidification takes place at an exceedingly slow rate. The high cooling rate in the melt-spinning technique makes the time enough for diffusion insufficient to yield a solid alloy that is homogeneous in composition.

In other words, solidification under non-equilibrium conditions will yield an alloy with composition far from uniform [1]. Heat transfer and fluid flow, in view of the various and complicated boundary conditions related to solidification process, affect the type of distribution and the scale of inhomogeneities of the solid product. The concentration distribution of a solute in the solid is determined by solute transport in the liquid which depends on the thermal fluid flow through the environment near the interface. Solidification inhomogeneities may be due to the segregation of the different elements forming the alloy during solidification of castings and ingots. The process of rapid solidification leads to the formation of amorphous and fine microstructures [2], new intermetallic phases [3] and anomalous vacancy concentrations [4, 5]. Deformation immediately after quenching facilitates the diffusion of excess quenched in vacancies. SnPb solder had been used as electronic interconnect materials for its outstanding electrical, chemical and mechanical properties. However, due to the toxic nature of Pb which imposes harm to the environment and living organisms, its utilization has been legislated below 0.1 wt% (1000 ppm) in the product according to European Union restriction of Hazardous substances (RoHS) since 2006. However, Pb and Pb compounds have been cited by the environmental protection agency (EPA) as one of the top 17 chemicals poisoning the greatest threat to human beings and the environment [6]. The European Union directives on waste electronic and electrical equipment (WEEE) and the restriction of hazardous substances (RoHS) stipulate that electronic equipment sold to European consumers be Pb-free as of 1 July 2006 [7, 8]. Therefore, the traditional Sn–Pb solders have been replaced with many kinds of Pb-free solders. Many lead-free solder alloys have already been proposed as alternatives for the conventional eutectic Sn–37Pb, and

✉ Rizk Mostafa Shalaby
rizk1969@yahoo.co.uk

¹ Metal Physics Laboratory, Physics Department, Faculty of Science, Mansoura University, P.O. Box 25516, Mansoura, Egypt

many of them have already been widely investigated [9–22]. In general, taking cost of raw metals into consideration, the majority of lead-free solders cost about two or three times more than Sn–Pb solders mainly for the reason that many of these new alloys contain valuable and expensive metals, such as silver. In contrast, the cost of Sn–0.7Cu eutectic solder is only about 1.3 times higher than that of Sn–Pb solder, which explains the reason that Sn–Cu has been successfully applied to practical production of consumer products [23]. Development of high strength Sn–0.7 Cu solders with the addition of small amount of Ag and In [24]. In this study, the effects of temperature and strain rate on the mechanical performance of Sn–0.7Cu, Sn–0.7–2Ag, Sn–0.72In and Sn–0.7Cu–2Ag–2In solders were investigated. The results showed that with the addition of Ag and In into Sn–0.7Cu, significant improvement in mechanical properties when compared with other commercially available Sn–0.7Cu solder alloy. With the increasing use of lead-free solder alloys in modern electronics, low melting materials are often required to protect the heat sensitive parts during soldering operation. Alloy systems based on Sn/Cu/Ag offer more reliable solutions and address the current problems involved with soldering process. A new method to reduce melting temperatures in Sn–Ag and Sn–Cu solder alloys [25]. The size dependent on melting properties of the eutectic alloys were studied by differential scanning technique and the results showed a reduction of 4.5 and 5 °C melting temperatures in the alloys when reduced from bulk to 92 and 96 nm sizes respectively. Mechanical properties and oxidation resistance performance improves by adding trace amount of elements such as; Ag [26], P [27] and Mo [28]. Chuang et al. [29] showed that by adding Ag into the Sn–Cu system, the melting temperature can be reduced from 227 to 217 °C. Hodulova et al. [30] observed that a small amount of Ni addition to lead-free solders produced more of the Cu₆Sn₅ phase during the reflow stage. The additions of trace amount Ni [31] and Sb into Sn–Cu solders are effective in achieving a lower of melting point while maintaining, or even improving the reliability of solder joints. In addition, Sn–Cu solder can also approach a lower melting point by means of doping low-melting elements such as Zn, Bi [32], Ga, and indium [33]. Therefore, further improvements in Sn–Cu solders are needed. Recent investigations have been stated that the presence of alloying elements in the solder has marked effects on the properties and performance of Sn–Cu solder joints. This paper outlines the main effects of rapid solidification and minor amount alloying element (In, Cr and Ni) on melting behavior, microstructure, and creep resistance of eutectic Sn–0.7 wt% Cu lead free solders produced by melt spun technique.

2 Experimental procedures

2.1 Sample preparation

Four alloys of compositions Sn–0.7 wt% Cu, Sn–0.7 wt% Cu–0.5 wt% In, Sn–0.7 wt% Cu–0.5 wt% Cr, and Sn–0.7 wt% Cu–0.5 wt% Ni were prepared by melting pure Sn, Cu, In, Ni and Cr (purity > 99.99 %). Required quantities of the used metals were weighed out and melted in a porcelain crucible using an induction furnace at 600 °C. After the alloys were molten, the melt was thoroughly agitated to effect homogenization. Then by ejecting the molten alloys on a rotating copper wheel (2900 rpm) which corresponds to a linear speed of 31.4 m/s of the melt-spinning technique. The resulting alloys have long ribbons form of about 100 μm in thickness and 1 cm width.

2.2 Sample characterization

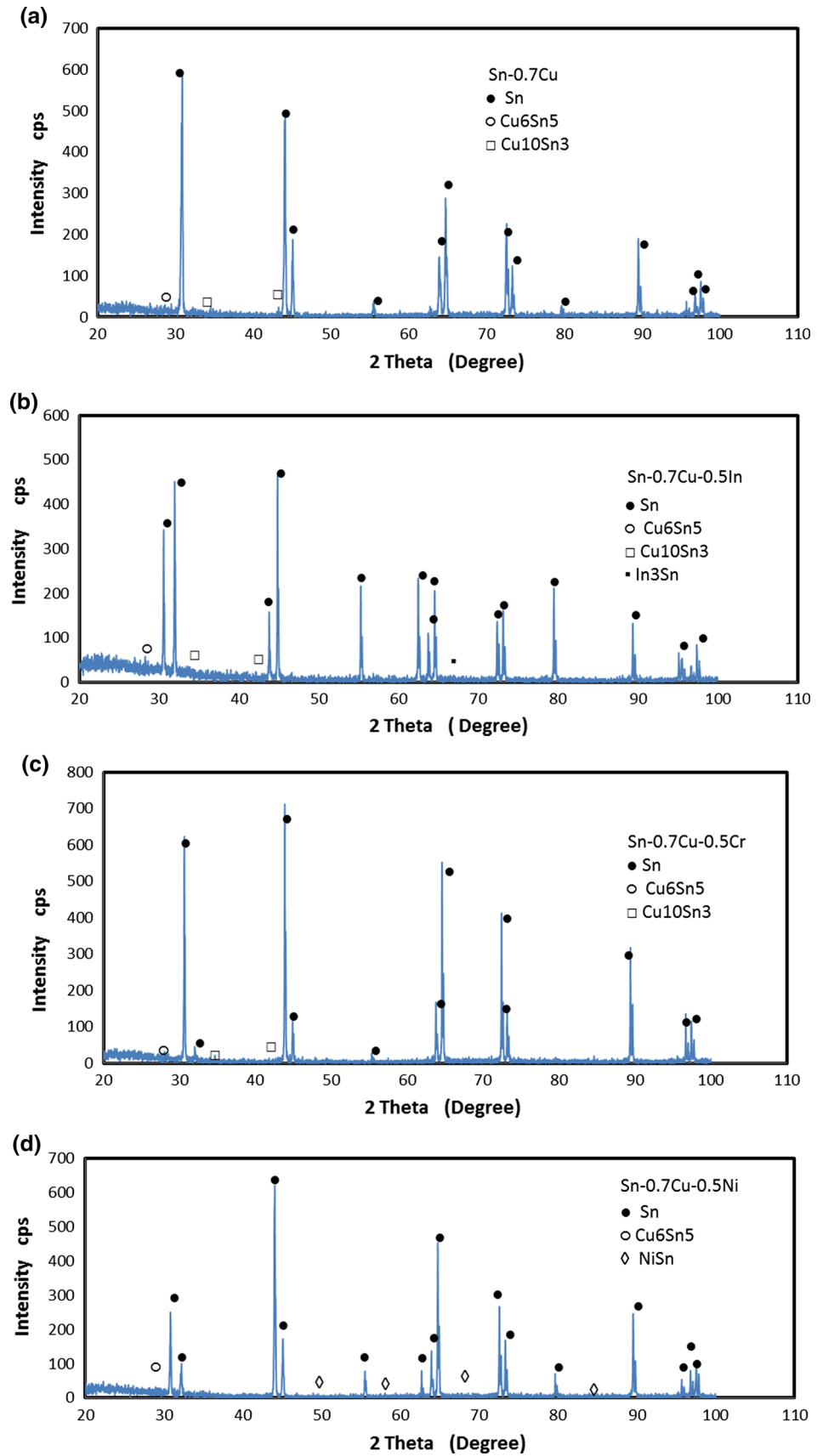
X-ray diffraction analysis was done on a Shimadzu X-ray diffractometer (DX-30), using Cu $k\alpha$ radiation ($\lambda = 1.54056\text{\AA}$) with Ni-filter was used to identify the structure of all produced alloys. The microstructure analysis was carried out on a scanning electron microscope (SEM) of type (JEOL JSM-6510LV, Japan) operate at 30 kV with high resolution 3 nm. Differential thermal analysis (DTA) was carried out on a (SDT Q600, USA) with a heat rate 10 K/min. The melting temperature of these alloys was determined by differential scanning calorimetry, with a heating rate 10 k/min. The measurement of resistivity is carried out by the double bridge method [34]. The dynamic young's modulus of melt spun alloys was examined by a dynamic resonance method [35–37]. The produced samples were tested in a Vickers microhardness tester, where a diamond pyramid indenter with square base is used and the Vickers hardness number is given by $HV = 0.185F/d^2$, where F is the applied load in N and d, is the average diagonal length in mm. Each reading was an average of at least ten measurements on the surface of the specimens. Micro-creep measurements as described elsewhere [38] were also carried out using a Vickers hardness tester using a fixed load of 0.49 N for dwell time up to 90 s.

3 Results and discussions

3.1 Structure

The XRD diffraction pattern for the as quenched Sn–0.7Cu, Sn–0.7Cu–0.5In, Sn–0.7Cu–0.5Cr and Sn–0.7Cu–0.5Ni melt spun alloys are shown in Fig. 1. For Sn–0.7Cu is shown in Fig. 1a contains pure β -Sn phase, Cu₆Sn₅, and

Fig. 1 The XRD patterns of as-quenched melt spun alloys: **a** Sn–0.7Cu, **b** Sn–0.7Cu–0.5In, **c** Sn–0.7Cu–0.5Cr, and **d** Sn–0.7Cu–0.5Ni



$\text{Cu}_{10}\text{Sn}_3$ intermetallic compound phases embedded in the Sn matrix. For Sn–0.7Cu–0.5In alloy Fig. 1b, the number of peaks of the Cu_6Sn_5 , intermetallic compound phase as the same while the results indicates the formation new intermetallic compounds $\beta\text{-In}_3\text{Sn}$ and $\text{Cu}_{10}\text{Sn}_3$ phases. For Sn–0.7Cu–0.5Cr alloy Fig. 1c, the number of peaks and intensity due to Cu_6Sn_5 increases. For Sn–0.7Cu–0.5Ni, Fig. 1d causes the presence of new intermetallic compound NiSn in addition to the Cu_6Sn_5 , and $\beta\text{-Sn}$ phases. The details of the XRD analysis are shown in Table 1. Table 1 shows the variation of axial ratio c/a with different compositions. It is found that the axial ratio increases to maximum value about 0.55015 Å at Sn–0.7Cu. The average grain size of Sn particles for all compositions was estimated from the diffraction peaks by using the Scherrer formula [39]: $d = 0.89\lambda/B \cos \theta$, where λ is the X-ray wavelength, B full width at half maximum (FWHM) of the XRD peak and θ is the diffraction angle. The results show that the value of particle size was observed for Sn–0.7Cu melt-spun alloy is 820 nm. It was also found that the addition of small amount of In, Cr and Ni at level 0.5 wt% to the eutectic Sn–0.7Cu alloy refines the effective grain size of $\beta\text{-Sn}$ phase and retains the fine dispersion of intermetallics precipitates in the $\beta\text{-Sn}$ matrix through the solidification process. Also the variations of the volume of the unit cell and the measured density have an opposite trend, in agreement with the following equation [40]: $\sum A = \delta v/1.6602$, where $\sum A$ is the sum of the atomic weight in the unit cell, δ is measured density in g/cm^3 and v is the volume of the unit cell in nm^3 .

3.2 Melting and thermal behavior

The melting point (T_m) of the solder alloy is a very crucial factor in the soldering process. The maximum temperature of soldering process is limited by the thermal properties of

components and devices on board, while the minimum is defined by the melting behavior of the solder and the requirement of forming a good joint with the substrate. These limitations often lead to the addition of third alloying elements in attempts to lower the melting points by a few degrees. The DSC curves obtained for the four alloys during heating with heating rate 10 K/min are shown in Fig. 2. The figure for all melt-spun alloys Sn–0.7Cu and Sn–0.7Cu–0.5X (X = In, Cr and Ni) shows a single endothermic peak corresponding to the melting reaction. From this figure the melting point (T_m), solidus temperature (T_s), Liquidus temperature (T_l), enthalpy of fusion (ΔH_f) and pasty range of these alloys were calculated in Table 2. For instance, the additions of trace amount In, Cr, and Ni into Sn–0.7Cu solders are effective in achieving a lower of melting point. In addition, Sn–0.7Cu solder can also approach a lower melting point by means of doping low-melting elements such as In. This reduction may be attributed to the decrease of the crystalline size, as observed in the work of Peter et al. [41–43]. The pasty range, which is the range between the solidus and liquidus temperatures, for the eutectic Sn–0.7Cu solder alloy is equal to zero. It becomes liquid at 226 °C, and solid at 226 °C, with a pasty or working range of degrees. This solder is called a eutectic alloy which means at 226 °C, we can go instantly from solid to liquid to solid just by applying or removing the heat source. It is primarily used to create dimensional effects in the solder itself and can be ‘pulled’ and manipulated to produce a variety of designs. While for the other solder alloys which contains minor additions at 0.5 wt% In, Cr or Ni exhibits an increase up to 13.48 °C. The solder in this range of temperature is a semi solid and has properties different from the solid or the liquid phases. The solder composed of 98.8 wt% Sn and 0.7 wt% Cu, 0.5 wt% In, it melts at 224.25 °C, but doesn’t become completely solid until it cools to 235.36 °C. This

Table 1 The details of the XRD analysis

Solder	Phases	Crystal system	Grain size (Å)	a (Å)	c (Å)	c/a
Sn–0.7Cu	$\beta\text{-Sn}$	Body centered tetragonal	560	5.788	3.1843	0.55015
	Cu_6Sn_5		474			
	$\text{Cu}_{10}\text{Sn}_3$		430			
Sn–0.7Cu–0.5In	$\beta\text{-Sn}$	Body centered tetragonal	340	5.8455	3.1770	0.54349
	Cu_6Sn_5		560			
	$\text{Cu}_{10}\text{Sn}_3$		420			
	In_3Sn		480			
Sn–0.7Cu–0.5Cr	$\beta\text{-Sn}$	Body centered tetragonal	480	5.8331	3.1815	0.54542
	Cu_6Sn_5		465			
	$\text{Cu}_{10}\text{Sn}_3$		660			
Sn–0.7Cu–0.5Ni	$\beta\text{-Sn}$	Body centered tetragonal	380	5.798	3.1691	0.54658
	Cu_6Sn_5		690			
	NiSn		620			

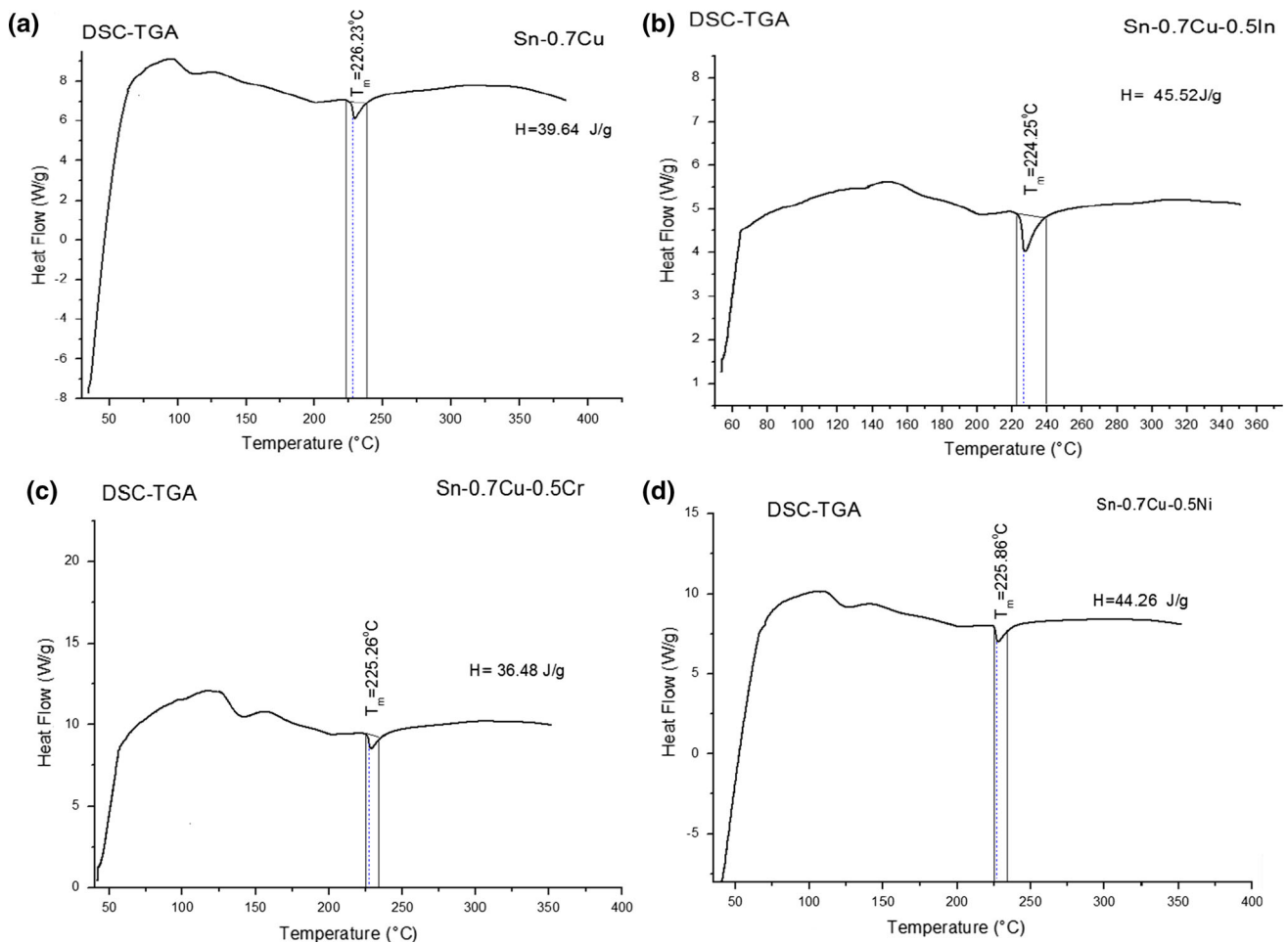


Fig. 2 Differential scanning calorimetry (DSC) melting curves for **a** Sn–0.7Cu, **b** Sn–0.7Cu–0.5In, **c** Sn–0.7Cu–0.5 Cr and **d** Sn–0.7Cu–0.5Ni solder alloys

Table 2 Thermal analysis

Solder	Onset temperature (°C)	Endset temperature (°C)	T_m (°C)	ΔH_f (J/g)	Pasty range (°C)
Sn–0.7Cu	226.23	226.23	226.23	45.52	Zero
Sn–0.7Cu–0.5In	223.63	235.36	224.25	39.64	11.73
Sn–0.7Cu–0.5Cr	224.50	236.2	225.26	36.48	11.70
Sn–0.7Cu–0.5Ni	224.45	237.93	225.86	44.26	13.48

means it has a “pasty range” or “working range” of 11.73 degrees. This solder is the best choice for copper foil work. The liquid temperature and narrow “pasty range” make it easy to form and maintain consistent high, rounded, beaded seams. Because of its relatively low melting point, lead-free solder is easy to rework to maintain a smooth finish solder bead.

The melting temperature for pure metals can be reduced when the particle size is decreased down to a few tens of nanometers; hence the attempt to lower the T_m with this

method of solder alloy has recently attracted more attention. As a result, the melting temperature of the nanoparticles solder can be an effective way to decrease the melting temperature. [43].

3.3 Stabilized and refined microstructure

The microstructure in Sn–Cu solder greatly influences the mechanical properties and in-service performance of the solder. For instance, ductility and creep behavior, the

fatigue performance and assembly reliability. The microstructures of the Sn–0.7Cu and Sn–0.7Cu–0.5X (X = In, Cr and Ni) solders was shown in Fig. 3. Figure 3a shows that the matrix contained Sn-rich phases, eutectic Sn–Cu phases and Cu–Sn intermetallics. It was indicated that the number of spherical Cu–Sn, In–Sn intermetallics increased with the In addition. It also noted that the Sn rich phase and spherical intermetallics were finer and similarly Fig. 3b. With small amount of Cr addition, a more refined microstructure of Sn–0.7Cu solder alloy has been obtained under the same cooling condition Fig. 3c. Figure 3d, illustrated the effects of Ni on the microstructure of as-cast Sn–0.7Cu solders. By adding a small amount of Ni element into the Sn–0.7Cu solder, the microstructure of the solder alloy is refined as well. The structure of Sn–0.7Cu–0.5In, Sn–0.7Cu–0.5Cr and Sn–0.7Cu–0.5Ni is refined compared to Sn–0.7Cu. Melt-spun ribbons was performed in air at high cooling rate, the microstructure of the Sn–0.7Cu–0.5Cr and Sn–0.7Cu–0.5Ni alloy are composed of two types of intermetallic phases, Cu_6Sn_5 and NiSn dispersed in a Sn-rich matrix.

3.4 Enhancement in mechanical properties

3.4.1 Young's modulus and microhardness

Thermal stresses in solder joints are unavoidable, and therefore it is important for solder alloys to be able to withstand the required thermal stresses. In addition, mechanical properties of Sn–Cu lead free solder can be various under different temperatures and strain rates. Sn–Cu alloys should have adequate mechanical strength such as tensile, shear and creep resistance. There is a continuous interest to better understand and improve mechanical properties of solder joint aiming to increase reliability. One frequently utilized way to influence properties of solder joint is to alloy either metallization (conductor) or solders with small amounts of additional elements. Effect of alloying elements on the mechanical properties of Sn–0.7Cu, is of significant practical importance. As shown in Table 3, it was found that Sn–0.7Cu alloy has an elastic modulus of about 60 Gpa. Indium additions can slightly influence the properties of Sn–0.7Cu solder alloy. The results showed that the hardness of Sn–

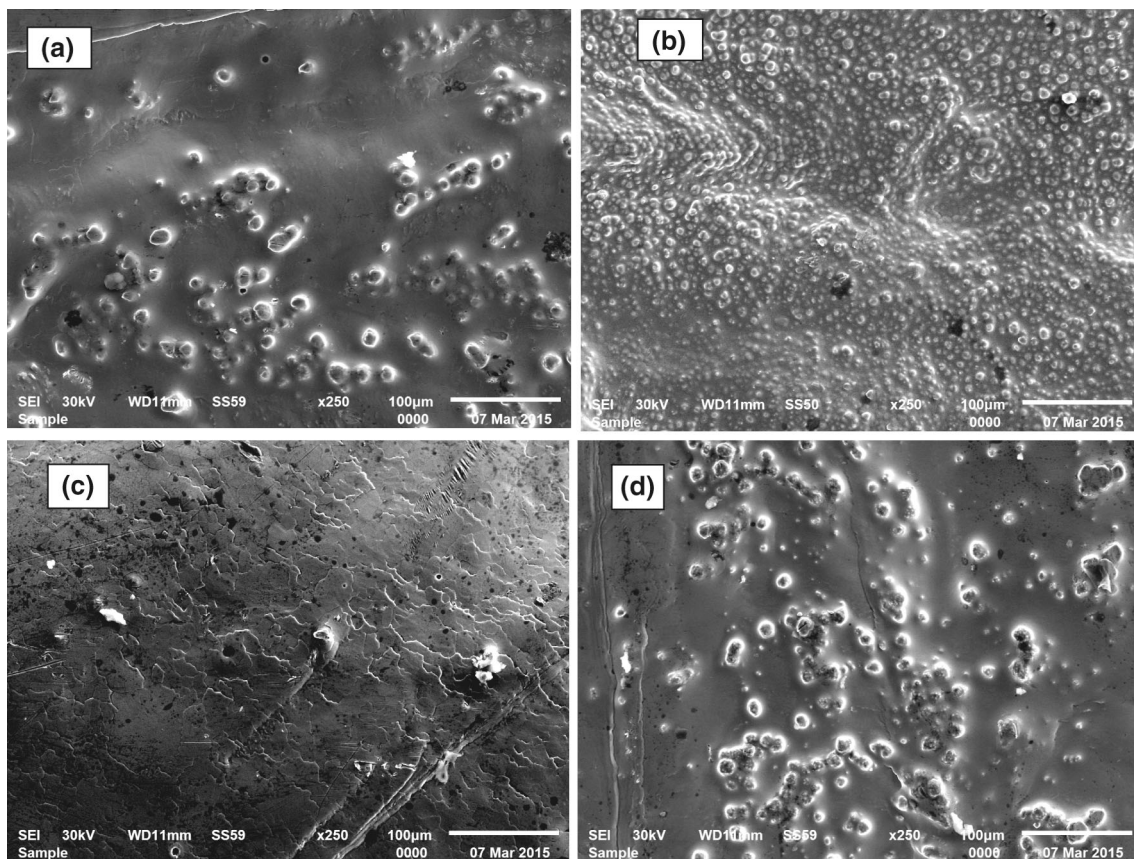


Fig. 3 SEM micrographs revealing the microstructures of **a** Sn–0.7Cu, **b** Sn–0.7Cu–0.5 In, **c** Sn–0.7Cu–0.5Cr and **d** Sn–0.7Cu–0.5Ni melt-spun alloys

Table 3 Young’s modulus and Vickers microhardness of Sn–0.7Cu and Sn–0.7Cu–0.5X (X = In, Cr and Ni) lead free solders

Solder	Young’s modulus (GPa)	Hv (MPa) 0.098 N and 10 s
Sn–0.7Cu	60.56	300.23
Sn–0.7Cu–0.5In	62.33	340.23
Sn–0.7Cu–0.5Cr	70.89	420.22
Sn–0.7Cu–0.5Ni	76.66	450.12

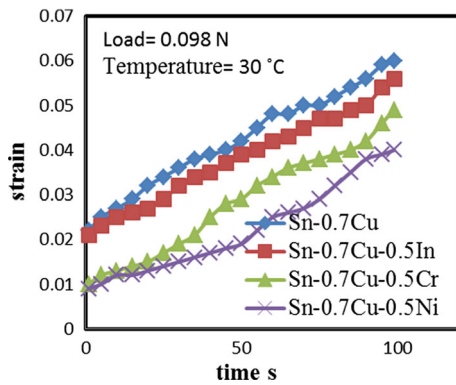


Fig. 4 The creep behavior of as-quenched Sn–0.7Cu, Sn–0.7Cu–0.5In, Sn–0.7Cu–0.5Cr and Sn–0.7Cu–0.5Ni lead free solder alloys

0.7Cu eutectic alloy was increased due to the addition of indium, chromium and nickel; however the creep resistance was increased as shown in Fig. 4.

3.4.2 Creep resistance

Creep is slow permanent deformation of a metal held for long periods of time under constant or slowly changing loads which are below its yield strength. The typical creep curve for a metal loaded has the trend illustrated by curves in Fig. 4. From such a curve it is evident that continued permanent deformation of a metal subsequent to the original application of a static load can be described in terms of two distinct stages of creep. In the first stage of creep curve (the initial primary, or diminishing rate stage), extension of the specimen occurs at a relatively high rate, but the creep rate diminishes constantly because of the strain hardening of the alloy. As the rate of creep decreases to an essentially constant value, the metal enters the second stage of creep (the secondary, constant-rate, or steady state stage). For the duration of the second stage, extension of the specimen continues at an approximately constant rate, either because strain hardening is almost exactly balanced by the reduction of cross-sectional area, or because the rate of resoftening (by recovery, etc.) balances the rate of strain hardening, or because deformation occurs by a peculiar mechanism, discussed below, which is directly affected by strain hardening, or because of complex interactions among all of these factors. In any case, the creep curve in this region approaches a straight line- evidently as an asymptotic approach from both sides to a point of inflection.

It is found in this work and others [44] that Hv decreases by increasing dwell time and since the hardness is given by $Hv = 0.102 F/s \text{ MPa}$, where F is the test load (N) and s is the surface area of an indentation (mm^2) and in this case the test load is kept constant at 0.098 N. Therefore, the increase in area (strain) with the indentation time under constant load by definition is creep. The strain here is considered as the fractional change in area and is given by $\text{strain} = \Delta S/S \%$, where $\Delta S = S - S_0$, and S_0 is considered to be the area at the minimum indentation time. The measurement of creep by this method is termed “micro-creep”; the term micro-creep comes from applying the stress to a very small area comparable to the area of a grain, and it is observed by microscope. Plotting the strain with indentation time, we obtain a typical creep curve, as shown in Fig. 4. Both Sn–0.7Cu, Sn–0.7Cu–0.5In, Sn–0.7Cu–0.5Cr and Sn–0.7Cu–0.5Ni alloys from 10 to 99 s exhibit the primary creep stage; however the creep resistance of Sn–0.7Cu–0.5In, Sn–0.7Cu–0.5Cr and Sn–0.7Cu–0.5Ni are higher than that of Sn–0.7Cu due to generate fine structure in the solder as a result of rapid solidification. Practically, it is found that resistance to deformation increases continuously, as grain size is reduced, as an approximately linear function of the logarithm of the mean free path along which slip can occur without interruption by grain boundaries, i.e., in a homogeneous alloy, as the logarithm of average grain diameter, neglecting twins. Further, because of the complex nature of the deformation process in polycrystalline alloys, aggregates strain harden more rapidly than single crystals, and fine grained aggregates more rapidly than coarse grained ones. Because it is more resistant to slip and strain hardens more rapidly, a fine grained alloy is in general and more resistant to impact than the same metal in a coarse-grained condition. For most engineering applications, however, the mechanical properties of a material are its most significant ones, and for such applications the fine-grained metals are preferred [45].

4 Conclusions

The present study proves that the rapid solidification technique is effective in studying the lead free solder alloys. The results show that nanostructured solders demonstrate size dependent melting properties and the

melting temperature. The results indicated that the melting temperature (T_m) of Sn–0.7Cu is modified to lower temperature by In, Cr and Ni additions. The formation of new intermetallic compounds such as In_3Sn , Cu_6Sn_5 , $\text{Cu}_{10}\text{Sn}_3$, and NiSn are more uniformly distributed inside Sn-rich phase effectively enhance the hardness and creep resistance of the eutectic Sn–0.7Cu solder joint at room temperature. It was found that the In, Cr or Ni addition has the effect of suppressing the formation of eutectic rapidly solidified Sn–0.7Cu alloy. The results of these tests are consistent with observed positive effect of the In, Cr and Ni in enhancing the performance of the eutectic Sn–0.7Cu solder as a practical lead-free solder.

Acknowledgments The author is grateful to Professor M. Kamal, Head of Metal Physics Laboratory, Physics Department, Faculty of Science, Mansoura University, Mansoura, Egypt, for his encouragement and cooperation.

References

- M. Kamal, J.C. Pieri, R. Jouty, *Mem. Sci. Rev. Met.* **PP**, 143–148 (1983)
- N.R. Green, J.A. Charles, G.C. Smith, *Mater. Sci. Technol.* **10**(11), 977 (1994)
- Q. Li, E. Johansen, L. Sarhoft-Kristesen, *J. Mater. Res.* **7**, 2756 (1992)
- G. Thomas, R.H. Willens, *Acta Metall* **13**, 139 (1965)
- G. Thomas, R.H. Willens, *Acta Metall* **14**, 138 (1966)
- D.Q. Yu, H.P. Xie, I. Wang, *J. Alloys Compd.* **385**, 119–125 (2004)
- M. Adtew, G. Selvaduray, *Mater. Sci. Eng. R Rep.* **27**, 95–141 (2000)
- N.S. Liu, K.L. Lin, *J. Alloys Compd.* **456**, 466–473 (2008)
- N. Lee *Mater. Advan. Packaging.* 181–218 (2008)
- K. Zeng, *JOM J. Miner. Metals Mater. Soc.* **61**(6), 28 (2009)
- K. Kim, S. Huh, K. Sugauma, *J. Alloys Compd.* **352**(1–2), 226–236 (2003)
- S.S. Babu, *Int. Mater. Rev.* **54**(6), 333–367 (2009)
- N. Chawla, *Int. Mater. Rev.* **54**(6), 368–384 (2009)
- S.W. Chen, C.H. Wang, S.K. Lin, C.N. Chiu, *J. Mater. Sci. Mater. Electron.* **18**(1–3), 19–37 (2007)
- Q.Z. Cui, F. Gao, S. Mukherjee, Z.Y. Gu, *Small* **5**(11), 1246–1257 (2009)
- Y.C. Lin, X. Chen, *J. Adhes. Sci. Technol.* **22**(14), 1631–1657 (2008)
- H. Ma, J.C. Suhling, *J. Mater. Sci.* **44**(5), 1141–1158 (2009)
- A. Micol, C. Martin, O. Dalverny, M. Mermet-Guyennet, M. Karama, *Microelectron. Reliab.* **49**(6), 631–641 (2009)
- E. Suhir, *Appl. Mech. Rev.* **62**(4), 4878–4885 (2009)
- M.J. Yim, Y. Li, K.S. Moon, K.W. Paik, C.P. Wong, *J. Adhes. Sci. Technol.* **22**(14), 1593–1630 (2008)
- L. Zhang, S.B. Xue, L.L. Gao, Z. Sheng, H. Ye, Z.X. Xiao, G. Zeng, Y. Chen, S.L. Yu, *J. Mater. Sci. Mater. Electron.* **21**(1), 1–15 (2010)
- L. Zhang, S.B. Xue, L.L. Gao, G. Zeng, Z. Sheng, Y. Chen, S.L. Yu, *J. Mater. Sci. Mater. Electron.* **20**(8), 685–694 (2009)
- C. Andersson, P. Sun, J. Liu, *J. Alloys Compd.* **457**(1–2), 97–105 (2008)
- A.A. El-Daly, A.E. Hammad, *J. Alloys Compd.* **509**, 8554–8560 (2011)
- R.N. Chukka, S. Telu, N.R.M.R. Bhargava, Chen L. J. *Mater. Sci. Mater. Electron.* **22**, 181–285 (2011)
- G. Zeng, S. Xue, I. Gao, I. Zhang, Y. Hu, Z. Lai, *J. Alloys Compd.* **509**, 7152–7162 (2011)
- G. Li, Y. Shi, H. Hao, Z. Xia, Y. Lei, F. Guo, *J. Alloys Compd.* **491**, 382–385 (2010)
- B.S.S. Chandra Rao, K.M. Kumer, V. Kripesh, K.Y. Zeng, *Mater. Sci. Eng. A* **528**, 4166–4172 (2011)
- T.H. Chuang, M.W. Wu, S.Y. Chang, S.F. Ping, I.C. Tsao, *J. Mater. Sci. Mater. Electron.* (2011). doi:10.1007/s10854-010-0253-1
- E. Hodulova, M. Pacut, E. Lechovic, B. Simekova, K. Ulrich, *J. Alloys Compd.* **509**, 7052–7059 (2011)
- T. Nishimura, S. Suenaga, M. Ikeda, Forth pacific rim international conference on advanced materials and processing I, 1087–1090 (2001)
- T. El-Ashram, R. Shalaby, *J. Electron. Mater.* **34**(2), 212–215 (2005)
- J. Hwang, Z. Guo, H. Koenigsmann, *Sold. Surf. Mount Technol.* **13**(2), 7–13 (2001)
- Y.A. Geller, A.G. Rakhshadt, *Sci. Mater.* **138**, 138–141 (1977)
- J.M. Ide, *Rev. Sci. Instrum.* **6**, 296 (1935)
- S. Sppinert, W.E. Teffit, *ASTM Proc.* **61**, 1221 (1961)
- E. Schreiber, O.L. Anderson, N. Soga, *Elastic Constants and Their Measurements* (McGraw Hill, New York, 1973), p. 82
- T. El-Ashram, R.M. Shalaby, *Electron. Mater.* **34**, 212 (2005)
- B.D. Cullity, *Elements of X-ray Diffraction*, 2nd edn. (Addison-Wesely, Reading, 1978), p. 248
- B.D. Cullity, *Elements of X-ray Diffraction*, 2nd edn (USA, 1959) ch. 10, p. 317
- A. Peters, B. Chung, C. Cohen, *Appl. Phys. Lett.* **71**, 2391 (1997)
- C. Zou, Y. Gao, B. Yang, Q. Zhai, C. Anderson, J. Liu, *Solder Surf. Mount Technol.* **21**(2), 9–13 (2009)
- R.N. Chukka, S. Telu, N.R.M.R. Bhargava, L. Chen, *J. Mater. Sci. Mater. Electron.* **22**(3), 281–285 (2011)
- R.M. Shalaby, *J. Mater. Electron.* **16**, 187 (2005)
- M.C. Smith, *Principles of Physical metallurgy* (Allied Pacific, Private Limited, 1962) Indian Addition, Printed in India by special arrangement with the original publishers, Harber and Brothers of New York and the copyright holders